EXPERIMENT OF HIGH RESOLUTION FIELD EMISSION IMAGING IN AN RF PHOTOCATHODE GUN

J. Shao[1], H. Chen, J. Shi, X. Wu, Tsinghua University, Beijing, China
M. Conde, W. Gai, G. Ha, E. Wisniewski, Argonne National Laboratroy, Lemont, IL 60439, USA
S.P. Antipov, S.V. Baryshev, C. Jing, Euclid Techlabs LLC, Bolingbrook, IL 60440, USA
F. Wang, SLAC National Accelerator Laboratory, Menlo Park 94025, CA, USA
[1]also at Argonne National Laboratroy, Lemont, IL 60439, USA

Abstract

The first *in situ* high resolution field emission (FE) imaging experiment has been carried out on an L-band photocathode gun test stand at Argonne Wakefield Accelerator facility (AWA). Separated strong emitters have been observed to dominate the field emission. Field enhancement factor, β, of small regions on the cathode has been measured with the imaging system. It is shown that most strong emitters overlaps with the high β regions. The post surface examinations reveal the origins of ~75% strong emitters overlap with the spots where rf breakdown have occurred. Detailed results are presented in this paper.

INTRODUCTION

Field emission (a.k.a dark current) plays an important role in high gradient dc and rf device, cold cathode electron sources, and internal electron transfer processes in electric devices [1]. To date, many question surrounding this fundamental physical phenomenon still remain, especially in rf case, resulting from the lack a means for *in situ* high resolution FE observation [2].

A method for high resolution dark current imaging has been proposed by selecting electrons from certain emitting phases with solenoids and a small aperture on a collimator [2, 3]. Based on the beam dynamics simulation, ~100 μm resolution is achievable with a 0.2 mm diameter aperture [3].

The first *in situ* high resolution dark current imaging experiment has been perform at AWA accordingly. With the imaging system, it is possible to measure field enhancement factor of small regions on the surface by fitting the luminous intensity and the electric field with the Fowler-Nordheim (F-N) equation [4]. After the experiment, the surface of the detachable cathode has been examined with scanning electron microscopy (SEM) and white light interferometer (WLI). Results from the dark current observation, the field enhancement factor measurement, and the surface examination have been analysis and compared.

EXPERIMENTAL SETUP

The upgraded L-band photocathode gun test stand at AWA is illustrated in Fig. 1. Diagnostics in the experiment are a bidirectional coupler to monitor the input and reflected rf power, an antenna (rf pickup probe) to monitor the rf signal inside the cavity, and a mirror to roughly locate the breakdown position during the rf conditioning. The YAG screens are placed perpendicular to the beam line and the image is transported out of the beam line in the transverse direction by a mirror angled at 45° and located behind each screen. A PI-MAX intensified CCD (ICCD) camera is used to capture the image on the last YAG screen. The image brightness can be also improved by the build-in frame accumulation function of the camera [2].

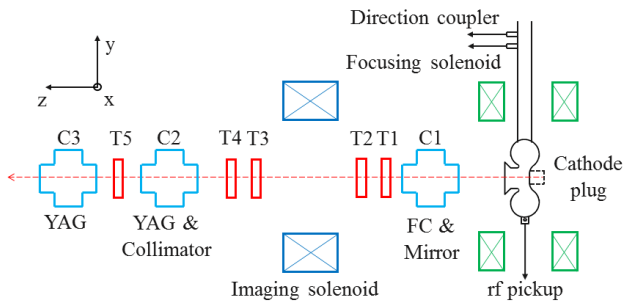

Figure 1: The L-band photocathode gun test stand at AWA. C, vacuum cross; T, trim; FC, Faraday cup; and YAG, doped Yttrium Aluminium Garnet phosphor screen.

Four 60 μm thick apertures at a 30 mm spatial interval are mounted on a stainless steel plate which can be precisely moved along the transverse direction by a motorized actuator so as to choose different apertures. The diameters of the apertures are 8 mm, 1 mm, 0.5 mm, and 0.2 mm, respectively. Based on the beam dynamics simulations, 40-140 μm resolution can be achieved depending on the initial FE electron emittance when the smallest aperture is applied [3].

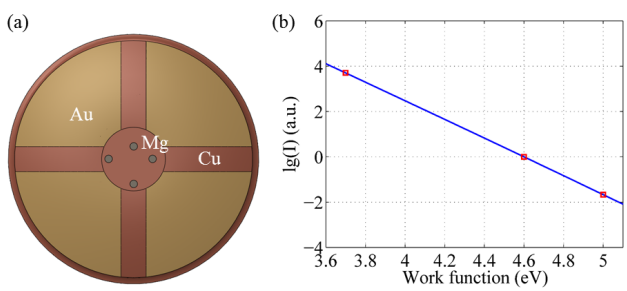

Figure 2: Cathode sputtering. (a) The pattern on the cathode by sputtering. (b) The emitting current density for materials with different work function. The three red squares indicate Mg, Cu, and Au, respectively.

A copper cathode has been applied in the experiment. The cathode is 20 cm in diameter with a large edge rounding and a small at centre. ~100 nm thick magnesium and

ISBN 978-3-95450-147-2

gold (Mg has a work function of 3.7 eV, Au 5.1 eV, and Cu 4.6 eV) have been sputtered in certain areas on the cathode to create a special pattern as reference, as illustrated in Fig. 2(a). When the localized surface E-field is 8-10 GV/m (the macroscopic surface E-field times the localized field enhancement factor), there will be orders of magnitude difference of the emitting current between these regions with different materials according to the F-N equation [4], as illustrated in Fig. 2(b).

EXPERIMENTAL RESULTS

Before the imaging experiment, the macroscopic surface E-field (noted as E_c) has been carefully conditioned to 120 MV/m with ~2.5 MW input power and 6.5 μs pulse length. Judged by the flash observed on the mirror, breakdowns occurred on the cathode and inside the cavity. After the conditioning, E_c was lowered to 105 MV/m. Steady dark current emission regions on the metal surface were observed and no further breakdowns occurred on those areas.

Other than FE electrons through the aperture, the brightness on the YAG screen also can be affected by the background luminance originating from X-rays generated by the energetic electrons, secondary electrons, light reflection along the beam line, etc. To quantify the background, dark current images were taken with a blank stainless steel plate. Then the background is subtracted from the image taken with the aperture present to ensure that the change of luminance value is only caused by the FE current through the aperture, as illustrated in Fig. 3.

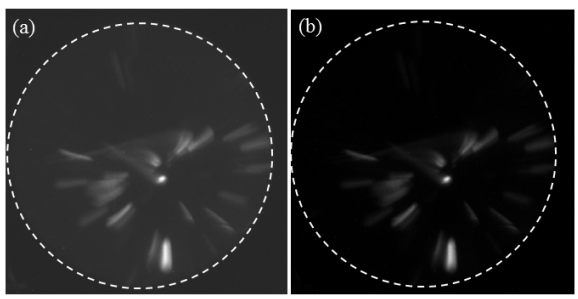

Figure 3: Dark current imaging with the 8 mm diameter aperture (accumulation of 20 frames). The white dashed circle indicates the boundary of the YAG screen. (a) Original image with the background. (b) After subtracting the background.

Dark current images on the last YAG screen with different apertures are shown in Fig. 4. The imaging quality improves with smaller apertures, which validates the high-resolution dark current imaging method in rf structures by emitting phase and energy selection.

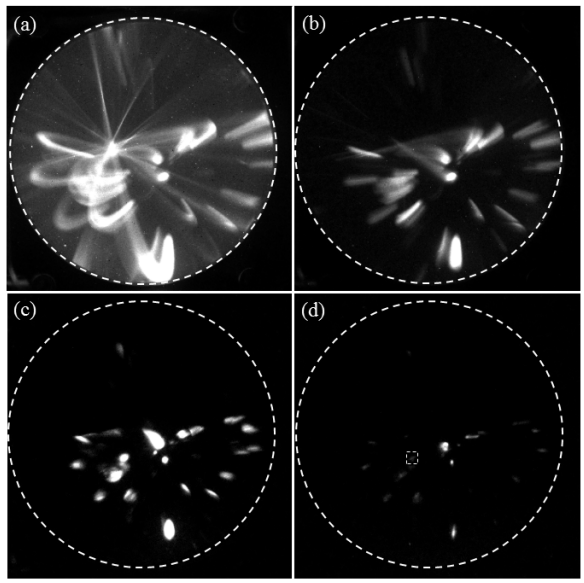

Figure 4: Dark current imaging with different apertures. The white dashed circle indicates the boundary of the YAG screen. The white dashed square in (d) indicates the emitter for the resolution calculation. (a) Without collimator. (b-d) With collimator. The aperture diameters are 8 mm, 1 mm, and 0.2 mm, respectively. (a-b) Accumulation of 20 frames. (c-d) Accumulation of 100 frames.

Based on beam line parameters for the images shown in Fig. 4, the average emitting phase of the electrons that can pass through the aperture, the magnification, and rotation from the cathode to the last YAG screen have been simulated to be 88°, 5.0, and 155°, respectively. The root-mean-square sizes of these emitters are determined by their actual sizes on the cathode as well as the system resolutions. Taking a small emission area as marked by the white dashed square in Fig. 4(d), the radial and angular system resolution are calculated to be better than 147 μm and 107 μm, respectively.

The field enhancement factor is a critical parameter in field emission study as it is considered to indicate the surface condition. In previous studies of rf structures, β is usually measured as an average value for a large surface. With the imaging system, β can further measured for localized regions by quantifying their variation in luminous intensity with the rf field.

The brightness of the dark current image is proportional to the energy deposited on the YAG screen (luminance of the YAG screen has a linear response to the deposited energy). β of selected areas can be obtained by fitting to the F-N equation. During the measurement, E_c was varied from 105 MV/m to 70 MV/m and the imaging solenoid current was adjusted accordingly to maintain the same emitting positions on the last YAG screen. The 8 mm diameter aperture was applied in this measurement to minimize the dependence of the capture ratio on E_c.

β for the entire imaged area is 76 which falls into the typical range in previous studies. The variation of β becomes more significant when smaller regions are selected, as illustrated in Fig. 5. Most strong emission regions

ISBN 978-3-95450-147-2

overlap with high β areas. A higher localized β may be obtained with an improved imaging resolution.

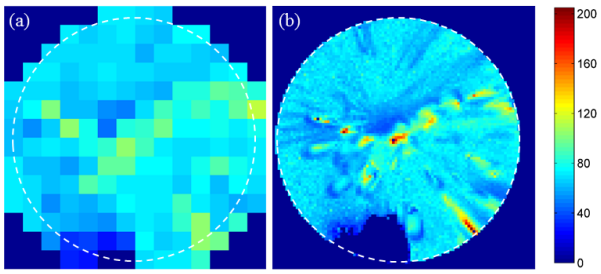

Figure 5: Mapping of field enhancement factor on the cathode. The white dashed circle indicates the boundary of the YAG screen. β is set to zero for regions with non-linear dependence in the F-N plot. The size of select regions is 610 μm × 610 μm and 94 μm × 94 μm on the cathode for (a) and (b), respectively.

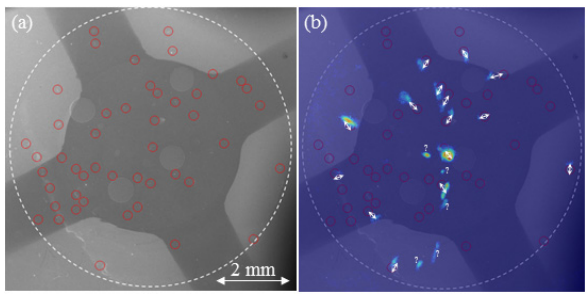

Figure 6: Overlap of strong dark current emitters and breakdown spots. (a) Overview of breakdown spots on the cathode. The red circles indicate the areas which contain breakdown spots. The white dash circle indicates the maximum visible range by the dark current imaging system. (b) Overlap of the strong dark current emitters and the breakdown spots. The dark current imaging is in false colour for better display. The overlapped emitters and breakdown spots are marked by arrows. The emitters with unknown origin are marked by the question mark.

After the imaging experiment, the cathode was examined by SEM and WLI. The major part of the surface remains intact after experiencing over hundreds of thousands of ~100 MV/m rf pulses. The roughness of the smooth areas is 10-20 nm. Meanwhile, ~40 breakdown spots have been observed within the areas as marked by the red circles in Fig. 6(a). Micro-structures such as melting craters and droplets are clearly signatures of the breakdown spots [4], which likely lead to high localized field enhancement. The microscopic valley deeper than 1 μm can be confirmed by the WLI. To study the relationship between the strong dark current emitters and the breakdown spots, the dark current image obtained with the smallest aperture has been resized and rotated based on the magnification and rotation from the cathode to the last YAG screen in beam dynamics simulation. The results show that ~75% of the strong emitters overlap with the breakdown spots, as illustrated in Fig. 6(b). The origin of the remaining ~25% strong emitters remains unknown. They may be attributed to microscopic surface features such as grain boundaries or defects that are not detected by the examination tools used. The results also reveal that half of the breakdown spots do not emit current at a level high enough to be detected by the imaging system.

The overlap of strong dark current emitters and breakdown spots with micro-structures supports the conventional understanding that FE may result from rf breakdowns in high gradient rf cavities. However the observation that no further breakdowns occurred at the strong dark current emitters imaged indicates that a steady FE alone may not be sufficient to trigger an rf breakdown.

CONCLUSION

The first *in situ* high resolution dark current emission imaging experiment has been performed at AWA. Separated emitters have been observed to dominate the field emission. The localized field enhancement factor has been measured. Post surface analysis by SEM and WLI reveals that ~75% strong dark current emitters overlap with the rf breakdown spots.

ACKNOWLEDGEMENT

We would like to thank the Tsinghua University machine shop for preparing the new shaped cathodes and all staff in the AWA group for their work in the experiment. The work by the AWA group is funded through the U.S. Department of Energy Office of Science under Contract No. DE-AC02-06CH11357. The work at Tsinghua University is supported by National Natural Science Foundation of China under Grant No. 11135004. The work by F.Y. Wang is supported by the U.S. Department of Energy Early Career Research Program under Contract Code LAB 11-572. SEM measurements were conducted in the Electron Microscopy Center of the Center for Nanoscale Materials at Argonne National Laboratory. Use of the Center for Nanoscale Materials, an Office of Science user facility, was supported by the U. S. Department of Energy, Office of Science, Office of Basic Energy Sciences, under Contract No. DE-AC02-06CH11357.

REFERENCES

[1] R. G. Forbes and J. H. Deane, "Reformulation of the standard theory of Fowler–Nordheim tunnelling and cold field electron emission", Proc. R. Soc. A 463, p. 2907, 2007.

[2] arXiv, http://arxiv.org/abs/1604.04086

[3] J. Shao, *et al.*, "Simulation of high resolution field emission imaging in an rf photocathode gun", presented at IPAC'16, Busan, Korea, May 2016, paper TUPOW014, this conference.

[4] J. W. Wang and G. A. Loew, "Field emission and rf breakdown in high-gradient room-temperature linac structures", SLAC, Menlo Park, USA, Rep. SLAC-PUB-7684, Oct. 1997.